

Dynamics of Fault Branching

James R. Rice and Renata Dmowska, Harvard University, Cambridge, MA 02138

16 November 2003

Reports

- Abercrombie, R. E., and J. R. Rice, "Can observations of earthquake scaling constrain slip weakening?", submitted to *Geophys. J. Int.*, September 2003, http://esag.harvard.edu/rice/AbercrombieRice_toGJI_03.pdf.
- Dmowska, R., J. R. Rice and N. Kame, "Fault branching and rupture directivity", *EOS Trans. AGU*, Fall Meet. Suppl., Abstract NG21B-0939, 2002.
- Fliss, S., H. S. Bhat, R. Dmowska and J. R. Rice, Fault jumping and bilateral propagation as a general mechanism of backward branching: Case study of transition from the Kickapoo to the Homestead Valley Fault in the 1992 Landers Earthquake, *EOS Trans. Amer. Geophys. Union*, vol. ??, no. ??, Fall Meet. Suppl., Abstract S41C-0101, 2003.
- Fliss, S., "Numerical elastodynamic modeling of earthquake rupture through branched and offset fault systems", internship report to École Polytechnique, France, of visiting student Sonia Fliss (advised by Bhat, Dmowska and Rice), August 2003, <http://esag.harvard.edu/fliss/reportweb.pdf>.
- Kame, N., J. R. Rice and R. Dmowska, "Effects of pre-stress state and rupture velocity on dynamic fault branching", *J. Geophys. Res.*, **108**(B5), *cn*: 2265, *doi*: 10.1029/2002JB002189, pp. ESE 13-1 to 13-21, May 2003, <http://esag.harvard.edu/dmowska/KRD.pdf>.
- Poliakov, A. N. B., R. Dmowska and J. R. Rice, "Dynamic shear rupture interactions with fault bends and off-axis secondary faulting", *J. Geophys. Res.*, **107** (B11), *cn*: 2295, *doi*:10.1029/2001JB000572, pp. ESE 6-1 to 6-18, November 2002, <http://esag.harvard.edu/dmowska/PDR.pdf>.
- Rice, J. R., C. G. Sammis and R. Parsons, "Off-fault secondary failures induced by a dynamic slip pulse", submitted to *Bull. Seismol. Soc. Amer.*, August 2003, http://esag.harvard.edu/rice/RiceSammisParsons_toBSSA03.pdf.

Progress

In studies reported last year, the main element of our progress was the work of *Kame, Rice and Dmowska* [*JGR*, 2003] on use of a numerical elastodynamic boundary integral equation (BIE) formulation that allowed for dynamically self-chosen rupture paths along branched fault systems that fail by Coulomb slip-weakening. The aim was to test and further elaborate theoretical guidelines of *Poliakov, Dmowska and Rice* [*JGR*, 2002] on when a rupture would follow a branch in a fault network. Our results confirmed that dynamic stresses around the rupture tip, which increase with increasing rupture velocity v_r at locations off the main fault plane, relative to those on it, could initiate rupture on a branching fault. They also showed that whether branched rupture could be continued to a larger scale depended on principal stress directions in the pre-stress state.

The most favored side for branching rupture switches from the extensional to the compressional side as we consider progressively shallower angles Ψ of the direction of maximum compressive pre-stress S_{max} with the main fault. Simultaneous rupturing on both faults, the main fault and the branch, can be activated when the branching angle ϕ is wide, but is usually difficult (except when v_r is very near the Rayleigh velocity) for a narrow branching angle, due to a strong stress interaction between faults. Comparisons (Kame *et al.* [2003]) with four field examples of branching in southern California suggested consistency with theoretical concepts and the numerical simulations. Those involved the 1971 San Fernando, 1979 Imperial Valley, 1985 Kettleman Hills, and 1992 Landers earthquakes.

In the continuing work reviewed here we have focused on observations of backward branching [Dmowska, Rice and Kame, EOS, 2002], Figure 1, applying the same numerical BIE formulation with Coulomb slip-weakening to test and refine theoretical concepts. Our work has focused most intensely on the rupture path transition from the Johnson Valley Fault (JVF) and Kickapoo Fault (KF) to the Homestead Valley Fault (HVF) in the 1992 Landers event [Fliss *et al.*, EOS, 2003].

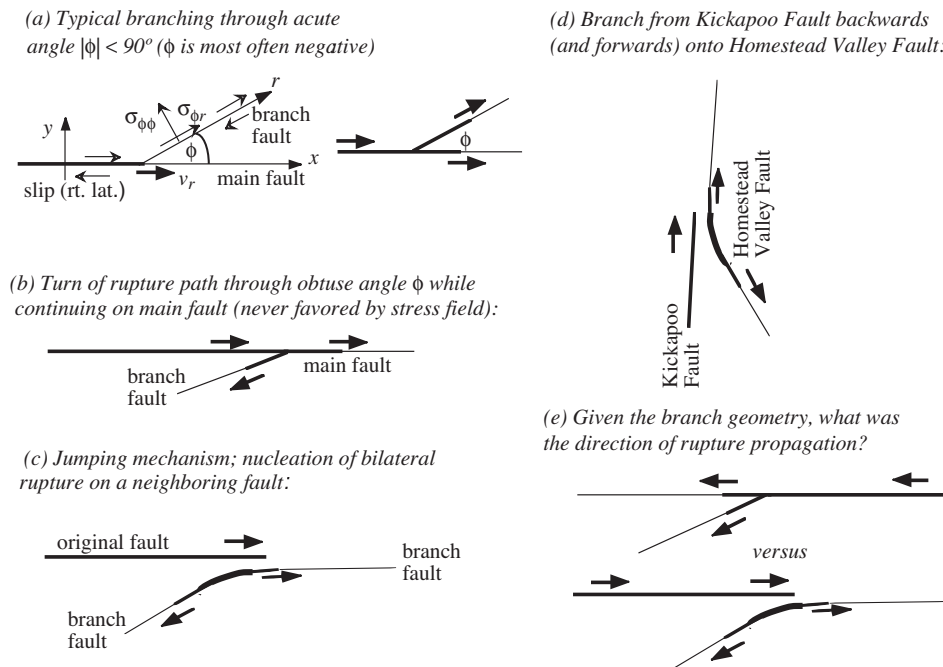


Figure 1 (Dmowska *et al.* [EOS, 2002]): Backward branching.

The importance of backward branching arises when we consider inferring the rupture directivity of past earthquakes from surface fault expressions, to aid seismic risk assessments for future events. Nakata *et al.* [*J. Geography*, 1998] propose to relate the observed surface branching of fault systems with the directivity of dynamic ruptures along them. Their work assumes that all branches are through acute angles in the direction of rupture propagation, like illustrated in Figure 1(a), and as is the case for the various branches analyzed in Kame *et al.* [2003]. However, as noted by Dmowska *et al.* [2002], in some observed cases rupture paths seem to branch through an obtuse angle ϕ , with $|\phi|$ well over 90° , as if to propagate "backwards", Figure 1(b,c).

We have collected four cases of such backward branching [Dmowska *et al.*, 2002], three as separate transitions of rupture path in the 1992 Landers earthquake, and one in the 1999 Hector Mine earthquake. Here we focus on the case in the Landers event when rupture crossed from the JVF to the HVF via the KF; see Figures 1(d) and 2. The rupture from the KF progressed not just forward onto the northern stretch of the HVF, but also backwards, i.e., SSE along the HVF [Spotila and Sieh, 1995; Sowers *et al.*, 1994; Zachariassen and Sieh, 1995; Rockwell *et al.*, 2000]. Measurements of surface slip along that backward branch (e.g. Sowers *et al.* and Spotila and Sieh) show right-lateral slip, decreasing towards the SSE. The length of the backward rupture stretch is around 4 km, so it is a prominent feature.

The field examples of such strongly obtuse branches suggest that there may be no simple correlation between fault geometry and rupture directivity. We have shown that a backward branch could not plausibly involve a rupture path which directly turned through an obtuse angle (while continuing also on the main fault), like illustrated in Figure 1(b). Stress fields [Poliakov *et al.*, 2002; Kame *et al.*, 2003] near a dynamic mode II crack are never consistent with continued right-lateral rupture through such obtuse branching angles. We argue instead that the backward branching involved a step-over of the rupture by nucleation on a neighboring fault and then bilateral propagation along it, Figure 1(c,d), similar to the way that Harris and Day [1993] described rupture transfer between parallel offset fault segments.

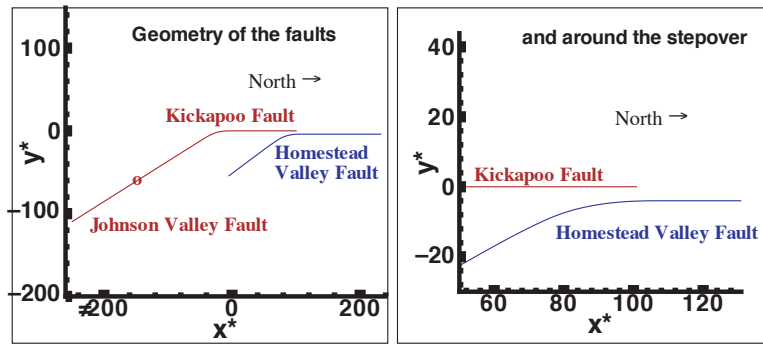


Figure 2: Geometry of stepover from the JVF-KF system to the HVF, for BIE modeling. Space coordinates are scaled as $(x^*, y^*) = 3(x, y) / R_0^o$, where R_0^o is the size of the slip-weakening zone, in the limit of low rupture propagation speed, on the north-south fault segments.

Arguments for the necessity of a jumping mechanism are as follows: Mapping of slip in the vicinity of the KF to HVF transition [Sowers *et al.*, 1994] shows that there is no connection of slip on the two faults at the surface. Li *et al.* [1994] used studies of fault zone trapped waves to show that there was transmission in a channel along the HVF, and in another channel along the Southern JVF and the KF, but no communication between those channels. Also, Felzer and Beroza [1999] showed through aftershock relative relocations that a separated fault surface geometry like in Figures 1(d) and 2 continued to the seismogenic depth.

By modeling of dynamic slip-weakening ruptures using the procedures of Kame *et al.* [2003], we have confirmed the strong plausibility of that mechanism of jumping and bilateral propagation as the mechanism of backward branching. Figure 2 shows the geometry of the model we examined. Figure 3 shows snapshots from the BIE results for slip velocities as a rupture propagates along the

JVF-KF system, stops at the termination of the KF, radiates out stress increases which trigger rupture on the HVF, and then propagates bilaterally on the curved HVF. The results lead us to conclude that to be able to infer the directivity of past events from a branched fault geometry, it will be necessary to have characterizations of fault geometry in the vicinity of the branch that are good enough to distinguish the two alternative scenarios shown in Figure 1(e).

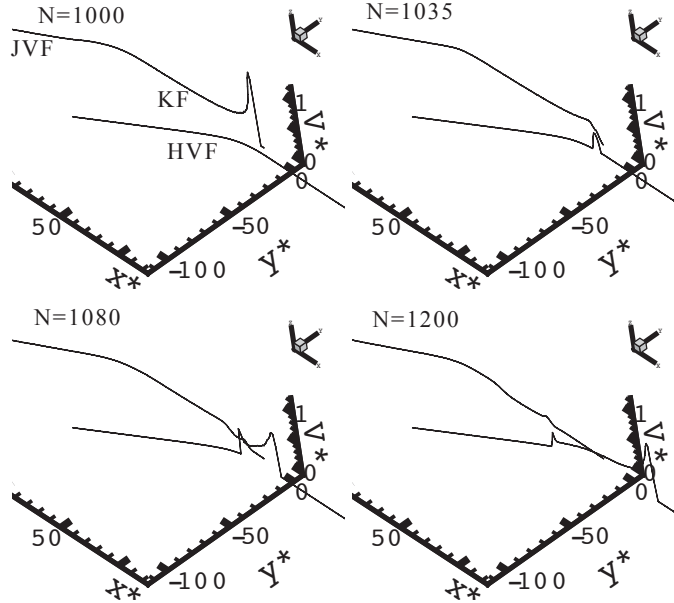


Figure 3: Near step-over view of transition of rupture from the JV-Fault (JVF)-KF system to the HVF, starting at a time just before rupture reaches the end of KF. Shows Harris-Day jump of the offset to the HVF and initial phase of bilateral rupture on the HVF, including along its curved part to the southeast (i.e., to form the backward branch). Slip rate V , in form $V^* = \mu V / (-\sigma_{yy}^o c_p)$, is shown along faults, whose traces are located in the plane of scaled space coordinates $(x^*, y^*) = 3(x, y) / R_0^o$. Pre-stress angle $\Psi = 30^\circ$ with the KF. Seismic S ratio chosen as 1.65 on north-south segments (and is larger on others), assuring that the rupture speed v_r remains sub-Rayleigh for the fault lengths modeled. Here $N = 4c_p t / R_0^o$ denotes the number of time steps into the calculation. We have verified that truncation of the JVF to the southeast and HVF to the north has no effect on the jump and negotiation of the bend in the HVF.

In other work, done in collaboration with Charles Sammis of USC, we have further developed our understanding of the relation between off-fault stressing near dynamic rupture tips and the activation of secondary failures in damage zones bordering faults [Rice, Sammis and Parsons, submitted to *BSSA*, 2003]. See Figure 4.

Also, two new approaches have been developed for inferring fracture energy, including its variation with earthquake slip, from seismic observations. One is based on fitting seismic slip inversions for the seven earthquakes of *Heaton* [PEPI, 1990] to the model of a propagating slip pulse [Rice et al., 2003]. That gives a broad range, $G = 0.1$ to 9 MJ/m^2 , with average in the range

of 2-4 MJ / m², and a clear tendency for G to increase with slip in the event. The other, developed in collaborative work with Rachel Abercrombie of BU, uses results on seismic energy radiation, moment, stress drop and slip for a large collection of earthquakes [Abercrombie and Rice, submitted to *GJI*, 2003]. We are able to infer for each such event a parameter G' which, we argue, is always of size comparable to G and coincides with it when the final dynamic friction stress during the last increments of seismic slip is negligibly different from the final static stress (i.e., when there is negligible dynamic overshoot or undershoot). The results also show a clear tendency for G' to increase with slip in the event, at least for slips up to the order of 1 m.

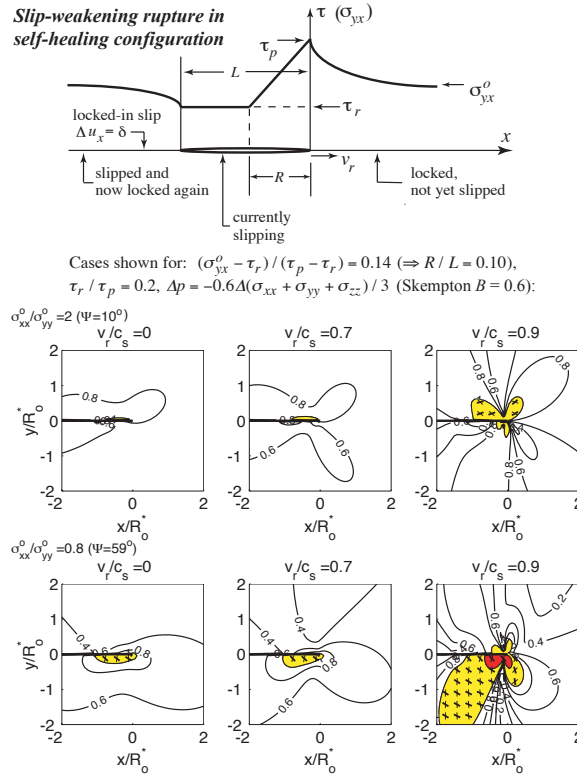


Figure 4 (Rice, Sammis and Parsons [2003]): Extending work of Poliakov *et al.* [2002], off-fault stresses are calculated for the steady-state dynamic self-healing pulse configuration, to estimate near-fault damage zones, for different pre-stress principal compression angles Ψ (the two rows) and rupture speeds v_r (the three columns). **YELLOW**: indicates near-fault stresses would cause Mohr-Coulomb shear failure. **RED**: indicates the greatest principal stress is tensile; would cause tensile failure. Shallow Ψ favors failure on compressional side at high v_r . Steep Ψ favors extensional side.